

Charm Mixing as Input for Model-Independent Determinations of Gamma.

Samuel Harnew, Jonas Rademacker

H H Wills Physics Laboratory, Bristol, UK

Abstract

We present a new method to constrain charm parameters at LHCb or the B factories that have so far only been accessible at the charm threshold. The coherence factor and average strong phase difference of D^0 and \bar{D}^0 decay amplitudes to the same final state, or equivalently, the average sine and cosine of the strong phase difference, play an important role in the precision determination of the CKM parameter γ using $B^\pm \rightarrow DK^\pm$ and related decay modes. So far, this crucial input from the charm sector could only be obtained from measurements based on quantum-correlated $D\bar{D}$ pairs produced at the charm threshold. We propose to constrain these parameters using charm mixing, using the very large charm samples available at the B factories and LHCb. We demonstrate for the example of $D \rightarrow K^+\pi^-\pi^+\pi^-$ that a substantial improvement in the precision of the coherence factor and average strong phase difference can be obtained with this method, using existing data.

1. Introduction

In this paper we present a novel method of constraining the coherence factor and average strong phase difference between D^0 and \bar{D}^0 decay amplitudes to the same multibody final state [1], or the average cosine and sine of this phase difference [2]. These parameters provide important input to the measurement of the CP -violating phase γ in $B^\pm \rightarrow DK^\pm$, $B^0 \rightarrow DK^*$ and similar decay modes¹, where the details of the analysis depend considerably

¹ CP -conjugate decays are always implied, unless stated otherwise. D stands for any superposition of D^0 and \bar{D}^0 .

on the final state of the subsequent D decay [3, 4, 5, 6, 7, 8, 9, 10, 11, 12, 13, 2, 14, 15, 16, 17].

So far, the charm interference parameters needed as input for γ measurements could only be obtained with data from the charm threshold. Current results exist from CLEO-c for $D \rightarrow K_S \pi^+ \pi^-$ and $D \rightarrow K_S K^+ K^-$ [15, 16] as well as $D \rightarrow K_S K^- \pi^+$ [13], $D \rightarrow K^+ \pi^- \pi^+ \pi^-$ and $D \rightarrow K^+ \pi^- \pi^0$ [18], with further improvements expected in the near future from BES III. These results provide important input to γ [14, 12, 19], but are statistically limited. Especially for $D \rightarrow K^+ \pi^- \pi^+ \pi^-$, uncertainties are quite large. This channel is particularly interesting as $B^\pm \rightarrow DK^\pm$ with $D^0 \rightarrow K^+ \pi^- \pi^+ \pi^-$ is potentially very sensitive to γ [5] and, as an all-charged final state, particularly suitable for LHCb [11]. In this paper we present a new method that will allow experiments such as LHCb, the B-factories, and their upgrades, to use their vast charm data samples to significantly improve the constraints on the coherence factor and average strong phase difference even without further input from the charm threshold – although the method we present would be even more powerful if combined with improved constraints from the charm threshold, for example from BES III.

The importance of data from the charm threshold as input for B physics is well established [1, 2, 14, 12, 19, 15, 16, 17]. The same input is also important for charm mixing and CP violation measurements [20, 21]. Charm threshold data are unique because they give access to well-defined superposition states of D^0 and \bar{D}^0 mesons, which allows the extraction of information inaccessible elsewhere, especially relating to the relative phases of D^0 and \bar{D}^0 decay amplitudes to the same final state.

Charm mixing [22, 23, 24, 25, 26, 27, 28] also provides well-defined D^0 - \bar{D}^0 superposition states, which in this case depend on the D decay time. In this paper we propose to exploit this feature to constrain the charm interference parameters, i.e. coherence factor and average strong phase difference for final states such as $K^- \pi^+ \pi^- \pi^+$, $K^- \pi^+ \pi^0$ and $K^- \pi^+ K_s^0$, or the average sine and cosine of the strong phase difference in the case of self-conjugate decays such as $D \rightarrow K_S \pi \pi$. We demonstrate the feasibility of such a measurement with a simulation study for the important example of $D \rightarrow K^+ \pi^- \pi^+ \pi^-$. Such measurements could be performed at any flavour factory that produces boosted D mesons of known initial flavour (e.g. from D^* decays), like the B^0 -factories, LHCb, and their upgrades, which in fact have access to vast numbers of such decays.

This paper is structured as follows: In Sections 2 and 3 we review the mixing formalism for multibody D decays, building on and extending the treatment presented in [20, 21]. We present a unified formalism for the interference effects in decays to self conjugate and non-self conjugate final states, and introduce the complex interference parameter, \mathcal{Z}^f . The coherence factor and average strong phase difference are the magnitude and phase of \mathcal{Z}^f , while the average cosine and sine of the strong phase difference are its real and imaginary part. In Sec. 4 we show how D -mixing can be used to constrain \mathcal{Z}^f . We present a simulation study demonstrating the feasibility of this approach, and demonstrate that with current LHCb data, substantial improvements in the precision of the coherence factor and strong phase difference for $D \rightarrow K^+\pi^-\pi^+\pi^-$ should be possible. Finally, in Sec. 6, we conclude.

2. Mixing Formalism

This section establishes the formalism for mixing in neutral D mesons. This is an extension to the formalism described in [20] and [21] allowing the application to the measurement of the complex interference parameter \mathcal{Z}^f , or equivalently the coherence factor and average strong phase difference of D^0 and \overline{D}^0 amplitudes for decays to non-self conjugate states, such as $D \rightarrow K\pi\pi\pi$ [1, 13, 18] or the average cosine and sine of the strong phase difference in decays to self-conjugate states such as $D \rightarrow K_S\pi^+\pi^-$ [2, 15, 16]. In the course of this, we establish a unified notation that treats decays to self-conjugate and non self-conjugate states on an equal footing.

The mixing of neutral D mesons occurs because the mass eigenstates $|D_1^0\rangle$ and $|D_2^0\rangle$ are not equal to the flavour eigenstates $|D^0\rangle$ and $|\overline{D}^0\rangle$, but linear superpositions of them:

$$\begin{aligned} |D_1\rangle &= p|D^0\rangle + q|\overline{D}^0\rangle \\ |D_2\rangle &= p|D^0\rangle - q|\overline{D}^0\rangle \end{aligned} \tag{2.1}$$

where p and q are complex numbers that satisfy $|q|^2 + |p|^2 = 1$. This general parametrisation is derived by assuming CPT invariance [29]. For our subsequent calculations, it is useful to define the following parameters related to q and p :

$$\lambda \equiv |\lambda| e^{-i\phi_{mix}} \equiv \frac{q}{p} \tag{2.2}$$

Both the phase and magnitude of λ are sensitive to CP violation in charm. The deviation of $|\lambda|$ from 1 is a measure of CP in D -mixing, while ϕ_{mix} is a convention-dependent quantity that is sensitive to CP violation in the interference between mixing and decay - usually, a phase convention is chosen where $\phi_{mix} = 0$ in the absence of CP violation.

The time evolution of the flavour eigenstates is governed by the Schrödinger equation:

$$-\frac{d}{dt} \begin{pmatrix} D^0 \\ \bar{D}^0 \end{pmatrix} = \mathbf{T}^{-1} \begin{pmatrix} M_1 + \frac{i}{2}\Gamma_1 & 0 \\ 0 & M_2 + \frac{i}{2}\Gamma_2 \end{pmatrix} \mathbf{T} \begin{pmatrix} D^0 \\ \bar{D}^0 \end{pmatrix}, \quad (2.3)$$

with

$$\mathbf{T} = \begin{pmatrix} p & q \\ p & -q \end{pmatrix}. \quad (2.4)$$

In Eq. 2.3 above, M_1 and M_2 refer to the masses of the mass eigenstates D_1^0 , D_2^0 respectively, whereas Γ_1 and Γ_2 refer to their widths. The matrix \mathbf{T} describes the linear transformation in Eq. 2.1 that maps the flavour eigenstates to the mass eigenstates. At this point it is useful to define the average D mass M and width Γ , as well as the mass and width difference, ΔM and $\Delta\Gamma$, as follows:

$$M \equiv \frac{M_1 + M_2}{2}, \quad \Gamma \equiv \frac{\Gamma_1 + \Gamma_2}{2}, \quad \Delta M \equiv M_2 - M_1, \quad \Delta\Gamma \equiv \Gamma_2 - \Gamma_1 \quad (2.5)$$

The usual dimensionless mixing parameters x and y are related to the above parameters as

$$x \equiv \frac{\Delta M}{\Gamma} \quad y \equiv \frac{\Delta\Gamma}{2\Gamma}. \quad (2.6)$$

Equation 2.3 allows us to calculate the time evolution of a D meson that is produced in a pure flavour eigenstate:

$$|D^0(t)\rangle = g_+(t)|D^0\rangle + \frac{q}{p}g_-(t)|\bar{D}^0\rangle \quad (2.7)$$

$$|\bar{D}^0(t)\rangle = g_+(t)|\bar{D}^0\rangle + \frac{p}{q}g_-(t)|D^0\rangle, \quad (2.8)$$

where $|D^0(t)\rangle$ refers to a state that was pure D^0 at $t = 0$, while $|\bar{D}^0(t)\rangle$ refers to a state that is purely \bar{D}^0 at $t = 0$. The time-dependent function $g_-(t)$ and

$g_+(t)$ are given by

$$g_+(t) = e^{-iMt - \frac{1}{2}\Gamma t} \cos\left(\frac{1}{2}\Delta Mt - \frac{i}{4}\Delta\Gamma t\right) \quad (2.9)$$

$$g_-(t) = e^{-iMt - \frac{1}{2}\Gamma t} i \sin\left(\frac{1}{2}\Delta Mt - \frac{i}{4}\Delta\Gamma t\right). \quad (2.10)$$

It is now useful to define the amplitudes for a flavour eigenstate to decay to a certain final state. For a decay to three or more particles, the final state is determined not only by the particle content, but also the position \mathbf{p} in phase space; for three-body decays such as $K^+\pi^-\pi^0$, \mathbf{p} is a point in the two-dimensional Dalitz plot, for four-body decays like $K^+\pi^-\pi^+\pi^-$ it is a point in a five-dimensional phase space, for 5-body decays the phase space is eight-dimensional etc. The corresponding point for the CP -conjugate final state, where all final state momenta and charges are reversed, is $\bar{\mathbf{p}}$. Denoting a final state with particle content f at point \mathbf{p} as $f_{\mathbf{p}}$, and the CP conjugate decay as $\bar{f}_{\bar{\mathbf{p}}}$, we define the following amplitudes:

$$\begin{aligned} \mathcal{A}(\mathbf{p}) &\equiv \langle f_{\mathbf{p}} | \hat{H} | D^0 \rangle & \bar{\mathcal{A}}(\bar{\mathbf{p}}) &\equiv \langle \bar{f}_{\bar{\mathbf{p}}} | \hat{H} | \bar{D}^0 \rangle \\ \mathcal{B}(\mathbf{p}) &\equiv \langle f_{\mathbf{p}} | \hat{H} | \bar{D}^0 \rangle & \bar{\mathcal{B}}(\bar{\mathbf{p}}) &\equiv \langle \bar{f}_{\bar{\mathbf{p}}} | \hat{H} | D^0 \rangle \end{aligned} \quad (2.11)$$

In terms of these, the time-dependent amplitudes for a flavour eigenstate at $t = 0$ to decay to a final state $f_{\mathbf{p}}$ or $\bar{f}_{\bar{\mathbf{p}}}$ at time t are given by:

$$\langle f_{\mathbf{p}} | \hat{H} | D^0(t) \rangle \equiv g_+(t)\mathcal{A}(\mathbf{p}) + \frac{q}{p}g_-(t)\mathcal{B}(\mathbf{p}) \quad (2.12)$$

$$\langle \bar{f}_{\bar{\mathbf{p}}} | \hat{H} | D^0(t) \rangle \equiv g_+(t)\bar{\mathcal{B}}(\bar{\mathbf{p}}) + \frac{q}{p}g_-(t)\bar{\mathcal{A}}(\bar{\mathbf{p}}) \quad (2.13)$$

$$\langle \bar{f}_{\bar{\mathbf{p}}} | \hat{H} | \bar{D}^0(t) \rangle \equiv g_+(t)\bar{\mathcal{A}}(\bar{\mathbf{p}}) + \frac{p}{q}g_-(t)\bar{\mathcal{B}}(\bar{\mathbf{p}}) \quad (2.14)$$

$$\langle f_{\mathbf{p}} | \hat{H} | \bar{D}^0(t) \rangle \equiv g_+(t)\mathcal{B}(\mathbf{p}) + \frac{p}{q}g_-(t)\mathcal{A}(\mathbf{p}) \quad (2.15)$$

To find the total decay rates to a given set of particles, the amplitudes given in Eqs. 2.12 - 2.15 are squared then integrated over phase space. We therefore

define the following integrals over the squared amplitudes:

$$\begin{aligned}
\int_{\Omega} \mathcal{A}(\mathbf{p})\mathcal{A}^*(\mathbf{p})d\mathbf{p} &\equiv \mathcal{A}^2 & \int_{\bar{\Omega}} \bar{\mathcal{A}}(\bar{\mathbf{p}})\bar{\mathcal{A}}^*(\bar{\mathbf{p}})d\bar{\mathbf{p}} &\equiv \bar{\mathcal{A}}^2 \\
\int_{\Omega} \mathcal{B}(\mathbf{p})\mathcal{B}^*(\mathbf{p})d\mathbf{p} &\equiv \mathcal{B}^2 & \int_{\bar{\Omega}} \bar{\mathcal{B}}(\bar{\mathbf{p}})\bar{\mathcal{B}}^*(\bar{\mathbf{p}})d\bar{\mathbf{p}} &\equiv \bar{\mathcal{B}}^2
\end{aligned} \tag{2.16}$$

Where the integrals containing $\mathcal{A}(\mathbf{p})$ and $\mathcal{B}(\mathbf{p})$ run over the phase space volume Ω , and the ones containing $\bar{\mathcal{A}}(\bar{\mathbf{p}})$ and $\bar{\mathcal{B}}(\bar{\mathbf{p}})$ run over $\bar{\Omega}$, the equivalent, CP -conjugate volume in the phase space of $f_{\bar{\mathbf{p}}}$. These volumes can be associated with the entire kinematically allowed region of phase space, or any sub-volume of this, which is important for binned analyses as in [2]. Throughout this note $*$ is used to denote the complex conjugate, whereas $\bar{}$ is used to denote the CP conjugate. We will also need the integrals over the cross terms:

$$\frac{\int_{\Omega} \mathcal{A}(\mathbf{p})\mathcal{B}^*(\mathbf{p})d\mathbf{p}}{\mathcal{A}\mathcal{B}} \equiv \mathcal{Z}^f \qquad \frac{\int_{\bar{\Omega}} \bar{\mathcal{A}}(\bar{\mathbf{p}})\bar{\mathcal{B}}^*(\bar{\mathbf{p}})d\bar{\mathbf{p}}}{\bar{\mathcal{A}}\bar{\mathcal{B}}} \equiv \bar{\mathcal{Z}}^f . \tag{2.17}$$

In the following we will refer to \mathcal{Z}^f as the *complex interference parameter* for the final state f . The parameter $\bar{\mathcal{Z}}^f$ is its CP -conjugate. The magnitude of \mathcal{Z}^f is between 0 and 1. It gives a measure of how coherent $\mathcal{A}(\mathbf{p})$ and $\mathcal{B}(\mathbf{p})$ are over the volume Ω . The phase of \mathcal{Z}^f gives the average phase difference between the two amplitudes over Ω . In the absence of CP violation $\mathcal{Z}^f = \bar{\mathcal{Z}}^f$

The complex interference parameter \mathcal{Z}^f is related to the coherence factor R_D^f and averaged strong phase difference δ_D^f introduced in [1] through

$$\mathcal{Z}^f \equiv R_D^f e^{-i\delta_D^f}. \tag{2.18}$$

Especially for binned analyses in decays to self-conjugate final states such as $K_s\pi^+\pi^-$, these interference effects are usually parametrised instead by the cosine and sine of the strong phase difference, averaged over a given bin with index i , $\langle \cos \delta \rangle_i$ and $\langle \sin \delta \rangle_i$, or short, c_i and s_i . This formalism was originally introduced in [2], although with a slightly different definition for c_i and s_i than used here and in most other articles that subsequently applied this formalism, e.g. [19, 14, 15, 16, 21]. The c_i and s_i parameters are related to the complex interference parameter in bin i , \mathcal{Z}_i^f , through

$$\mathcal{Z}_i^f \equiv c_i + i s_i \tag{2.19}$$

Here, we will continue to use \mathcal{Z}^f as it unifies the formalism for decays to self-conjugate and non-self conjugate states. The subtle differences between decays to non self-conjugate and self conjugate decays are discussed further in Sec. 2.1 and Sec. 2.2.

We now show how mixing can be used to constrain the complex interference parameter \mathcal{Z}^f . Taking the magnitude-squared of the amplitudes given in Eqs. 2.12 - 2.15, and then integrating over phase space yields the following expressions for the time-dependent decay rates:

$$\begin{aligned} \Gamma(D^0(t) \rightarrow f)_{\Omega} = & \frac{1}{2} e^{-\Gamma t} \left[\mathcal{A}^2 (\cosh y\Gamma t + \cos x\Gamma t) \right. \\ & + \mathcal{B}^2 (\cosh y\Gamma t - \cos x\Gamma t) |\lambda|^2 \\ & + 2\mathcal{A}\mathcal{B} [Re(\mathcal{Z}^f \lambda) \sinh(y\Gamma t) \\ & \left. + Im(\mathcal{Z}^f \lambda) \sin(x\Gamma t)] \right] \end{aligned} \quad (2.20)$$

$$\begin{aligned} \Gamma(D^0(t) \rightarrow \bar{f})_{\bar{\Omega}} = & \frac{1}{2} e^{-\Gamma t} \left[\bar{\mathcal{B}}^2 (\cosh y\Gamma t + \cos x\Gamma t) \right. \\ & + \bar{\mathcal{A}}^2 (\cosh y\Gamma t - \cos x\Gamma t) |\lambda|^2 \\ & + 2\bar{\mathcal{A}}\bar{\mathcal{B}} [Re(\mathcal{Z}^{\bar{f}*} \lambda) \sinh(y\Gamma t) \\ & \left. + Im(\mathcal{Z}^{\bar{f}*} \lambda) \sin(x\Gamma t)] \right] \end{aligned} \quad (2.21)$$

$$\begin{aligned} \Gamma(\bar{D}^0(t) \rightarrow \bar{f})_{\bar{\Omega}} = & \frac{1}{2} e^{-\Gamma t} \left[\bar{\mathcal{B}}^2 (\cosh y\Gamma t + \cos x\Gamma t) \right. \\ & + \bar{\mathcal{A}}^2 (\cosh y\Gamma t - \cos x\Gamma t) \frac{1}{|\lambda|^2} \\ & + 2\bar{\mathcal{A}}\bar{\mathcal{B}} [Re(\mathcal{Z}^{\bar{f}}/\lambda) \sinh(y\Gamma t) \\ & \left. + Im(\mathcal{Z}^{\bar{f}}/\lambda) \sin(x\Gamma t)] \right] \end{aligned} \quad (2.22)$$

$$\begin{aligned} \Gamma(\bar{D}^0(t) \rightarrow f)_{\Omega} = & \frac{1}{2} e^{-\Gamma t} \left[\mathcal{B}^2 (\cosh y\Gamma t + \cos x\Gamma t) \right. \\ & + \mathcal{A}^2 (\cosh y\Gamma t - \cos x\Gamma t) \frac{1}{|\lambda|^2} \\ & + 2\mathcal{A}\mathcal{B} [Re(\mathcal{Z}^{f*}/\lambda) \sinh(y\Gamma t) \\ & \left. + Im(\mathcal{Z}^{f*}/\lambda) \sin(x\Gamma t)] \right] \end{aligned} \quad (2.23)$$

To achieve a more compact notation we introduce the function $\zeta(z)$ that acts on the generic complex number z as

$$\zeta(z) = y\text{Re}(z) + x\text{Im}(z). \quad (2.24)$$

Assuming terms of order 3 and higher in the mixing parameters x and y are negligible, leads to the following expressions:

$$\Gamma(D^0(t) \rightarrow f)_{\bar{\Omega}} \simeq e^{-\Gamma t} \left[\mathcal{A}^2 \left(1 + \frac{y^2 - x^2}{4}(\Gamma t)^2 \right) + \mathcal{B}^2 \left(|\lambda|^2 \frac{x^2 + y^2}{4}(\Gamma t)^2 \right) + \mathcal{A}\mathcal{B}\zeta(\mathcal{Z}^f\lambda)(\Gamma t) \right] \quad (2.25)$$

$$\Gamma(D^0(t) \rightarrow \bar{f})_{\bar{\Omega}} \simeq e^{-\Gamma t} \left[\bar{\mathcal{B}}^2 \left(1 + \frac{y^2 - x^2}{4}(\Gamma t)^2 \right) + \bar{\mathcal{A}}^2 \left(|\lambda|^2 \frac{x^2 + y^2}{4}(\Gamma t)^2 \right) + \bar{\mathcal{A}}\bar{\mathcal{B}}\zeta(\mathcal{Z}^{\bar{f}*}\lambda)(\Gamma t) \right] \quad (2.26)$$

$$\Gamma(\bar{D}^0(t) \rightarrow \bar{f})_{\bar{\Omega}} \simeq e^{-\Gamma t} \left[\bar{\mathcal{A}}^2 \left(1 + \frac{y^2 - x^2}{4}(\Gamma t)^2 \right) + \bar{\mathcal{B}}^2 \left(\frac{1}{|\lambda|^2} \frac{x^2 + y^2}{4}(\Gamma t)^2 \right) + \bar{\mathcal{A}}\bar{\mathcal{B}}\zeta(\mathcal{Z}^{\bar{f}}/\lambda)(\Gamma t) \right] \quad (2.27)$$

$$\Gamma(\bar{D}^0(t) \rightarrow f)_{\bar{\Omega}} \simeq e^{-\Gamma t} \left[\mathcal{B}^2 \left(1 + \frac{y^2 - x^2}{4}(\Gamma t)^2 \right) + \mathcal{A}^2 \left(\frac{1}{|\lambda|^2} \frac{x^2 + y^2}{4}(\Gamma t)^2 \right) + \mathcal{A}\mathcal{B}\zeta(\mathcal{Z}^{f*}/\lambda)(\Gamma t) \right] \quad (2.28)$$

So far, we have allowed for CP violation in all stages of this derivation. There are three distinct types of CP violation that could be present in these decays [29]:

- **Direct CP violation** - This is a difference between CP conjugate decay amplitudes at any point in phase space i.e. $\mathcal{A}(\mathbf{p}) \neq \bar{\mathcal{A}}(\bar{\mathbf{p}})$ or $\mathcal{B}(\mathbf{p}) \neq \bar{\mathcal{B}}(\bar{\mathbf{p}})$. In the absence of direct CP violation we have $|\mathcal{Z}^f| = |\bar{\mathcal{Z}}^f|$, $\mathcal{A} = \bar{\mathcal{A}}$ and $\mathcal{B} = \bar{\mathcal{B}}$.
- **CP violation in mixing** - This is when $|\lambda| \neq 1.0$. This implies that the probability of a $D^0 \rightarrow \bar{D}^0$ oscillation is not the same as a $\bar{D}^0 \rightarrow D^0$ oscillation.
- **CP violation in the interference between mixing and decay** It is related to the relative phase between the amplitude $D^0 \rightarrow f$ without mixing, and the amplitude for the same initial and final state, that proceeds via mixing (symbolically: $D \rightarrow \bar{D} \rightarrow f$). If this relative phase is different between CP conjugate processes it leads to CP violation, that predominantly manifests itself in time-dependent measurements (as the well-known $\sin 2\beta$ in the B_d^0 system). In terms of our formalism, this type of CP violation is characterised by $\arg(\mathcal{Z}^f \lambda) \neq \arg(\bar{\mathcal{Z}}^f / \lambda)$.

Following the usual phase convention, we set ϕ_{mix} to zero in the absence of CP violation in the interference between mixing and decay. This leads to the further constraint $\mathcal{Z}^f = \bar{\mathcal{Z}}^f$ in absence of direct CP violation.

In the following two subsections we look at the formalism in two specific scenarios; self-conjugate final states where $f_{\mathbf{p}} = \bar{f}_{\bar{\mathbf{p}}}$, and the regime where $\mathcal{A} \ll \mathcal{B}$.

2.1. Decays with $\mathcal{A} \ll \mathcal{B}$

This section takes the mixing formalism from Sec. 2 and applies the constraint that $\mathcal{A} \ll \mathcal{B}$. This is applicable for decays such as $D \rightarrow K^+ \pi^- \pi^+ \pi^-$, $D \rightarrow K^+ \pi^- \pi^0$, $D \rightarrow K^- \pi^+ K_s^0$ and $D \rightarrow K^- \pi^+$. \mathcal{A} and $\bar{\mathcal{A}}$ refer to the doubly Cabibbo-suppressed (DCS) amplitudes such as $D^0 \rightarrow K^+ \pi^- \pi^+ \pi^-$ and $\bar{D}^0 \rightarrow K^- \pi^+ \pi^- \pi^+$, while \mathcal{B} and $\bar{\mathcal{B}}$ refer to the corresponding Cabibbo-favoured (CF) amplitudes, i.e. in the above example to $D^0 \rightarrow K^- \pi^+ \pi^- \pi^+$ and $\bar{D}^0 \rightarrow K^+ \pi^- \pi^+ \pi^-$. In this scenario it is useful to make two further definitions related to the ratios of decay amplitudes:

$$r_{Df} \equiv \frac{\mathcal{A}}{\mathcal{B}} \qquad \bar{r}_{Df} \equiv \frac{\bar{\mathcal{A}}}{\bar{\mathcal{B}}} \qquad (2.29)$$

If \mathcal{A} and $\bar{\mathcal{A}}$ refer to DCS decays, and \mathcal{B} and $\bar{\mathcal{B}}$ to DCS decays, the magnitude of these parameters is $\sim \sin^2 \theta_c$, where θ_c is the Cabibbo angle. Substituting

these definitions into Eqs. 2.25 - 2.28 and neglecting terms of order 4 or higher in $x, y, r_{Df}, \bar{r}_{Df}$, we obtain the following expressions for the decay rates:

$$\Gamma(D^0(t) \rightarrow f)_{\Omega} \simeq \mathcal{B}^2 e^{-\Gamma t} \left[r_{Df}^2 + |\lambda|^2 \frac{x^2 + y^2}{4} (\Gamma t)^2 + r_{Df} \zeta(\mathcal{Z}^f \lambda) (\Gamma t) \right] \quad (2.30)$$

$$\Gamma(D^0(t) \rightarrow \bar{f})_{\bar{\Omega}} \simeq \bar{\mathcal{B}}^2 e^{-\Gamma t} \left[1 + \frac{y^2 - x^2}{4} (\Gamma t)^2 + \bar{r}_{Df} \zeta(\mathcal{Z}^{\bar{f}} \lambda) (\Gamma t) \right] \quad (2.31)$$

$$\Gamma(\bar{D}^0(t) \rightarrow \bar{f})_{\bar{\Omega}} \simeq \bar{\mathcal{B}}^2 e^{-\Gamma t} \left[\bar{r}_{Df}^2 + \frac{1}{|\lambda|^2} \frac{x^2 + y^2}{4} (\Gamma t)^2 + \bar{r}_{Df} \zeta(\mathcal{Z}^{\bar{f}} / \lambda) (\Gamma t) \right] \quad (2.32)$$

$$\Gamma(\bar{D}^0(t) \rightarrow f)_{\Omega} \simeq \mathcal{B}^2 e^{-\Gamma t} \left[1 + \frac{y^2 - x^2}{4} (\Gamma t)^2 + r_{Df} \zeta(\mathcal{Z}^{f^*} / \lambda) (\Gamma t) \right]. \quad (2.33)$$

The rates given in Eq. 2.30 and Eq. 2.32 are highly suppressed because the decays can only proceed via a DCS decay or a $D^0 - \bar{D}^0$ oscillation followed by a CF decay. The rates in Eq. 2.31 and Eq. 2.33 have no such suppression as both can proceed directly via a CF decay. We will follow the usual convention and refer to the suppressed decays described by Eq. 2.30 and Eq. 2.32 as “wrong sign” (WS) decays, while the favoured rates Eq. 2.31 and Eq. 2.32 are termed “right sign” (RS) decays. This is subtly different from the distinction between DCS and CF decays due to the effects of mixing. Fig. 1 shows an illustration of WS and RS decays for the decay mode $D^0 \rightarrow K^- \pi^+ \pi^- \pi^+$.

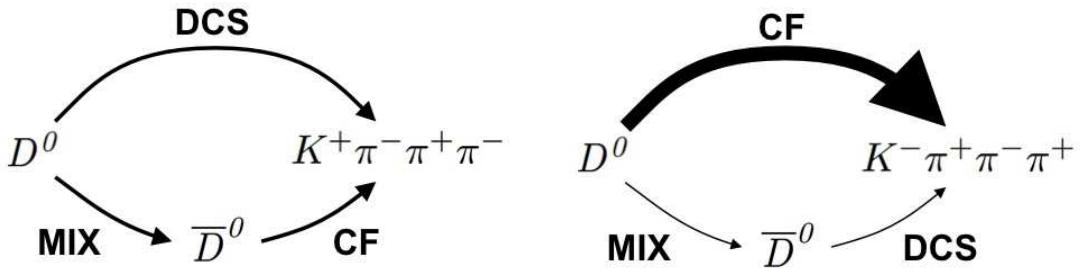


Figure 1: Illustration of “wrong sign” (WS) and “right sign” (RS) decays, pictured on the left and right respectively. Although this shows the specific example of $D^0 \rightarrow K^- \pi^+ \pi^- \pi^+$ it applies equally to all the decay modes listed in the text.

In the WS decays, the mixing-induced amplitude and the unmixed DCS amplitude are of comparable magnitude, making them ideal to study mixing and interference effects. RS decays on the other are completely dominated by the unmixed CF decay amplitude. A good experimental observable is the time dependent ratio of WS to RS decays. This takes advantage of the larger RS decay rate as a control channel, cancelling many efficiency effects in the detection and selection process. The time dependent ratio of WS to RS decays is given by

$$r_{\Omega}(t)^+ = \frac{\Gamma(D^0(t) \rightarrow f)_{\Omega}}{\Gamma(\bar{D}^0(t) \rightarrow f)_{\Omega}} \simeq r_{Df}^2 + r_{Df} \zeta(\mathcal{Z}^f \lambda) \Gamma t + |\lambda|^2 \frac{x^2 + y^2}{4} (\Gamma t)^2 \quad (2.34)$$

$$r_{\bar{\Omega}}(t)^- = \frac{\Gamma(\bar{D}^0(t) \rightarrow \bar{f})_{\bar{\Omega}}}{\Gamma(D^0(t) \rightarrow \bar{f})_{\bar{\Omega}}} \simeq \bar{r}_{Df}^2 + \bar{r}_{Df} \zeta(\mathcal{Z}^{\bar{f}}/\lambda) \Gamma t + \frac{1}{|\lambda|^2} \frac{x^2 + y^2}{4} (\Gamma t)^2 \quad (2.35)$$

In the absence of any source of CP violation the ratio of WS to RS decays simplifies to

$$r_{\Omega}(t) \simeq r_{Df}^2 + r_{Df} \zeta(\mathcal{Z}^f) \Gamma t + \frac{x^2 + y^2}{4} (\Gamma t)^2 \quad (2.36)$$

where $r_{\Omega}(t) \equiv r_{\Omega}(t)^+ \equiv r_{\bar{\Omega}}(t)^-$. The frequently used parameter $y' = y \cos \delta_D^f - x \sin \delta_D^f$ is related to the complex interference parameter \mathcal{Z}^f through:

$$y' = \frac{\zeta(\mathcal{Z}^f)}{|\mathcal{Z}^f|} = \frac{y \text{Re} \mathcal{Z}^f + x \text{Im} \mathcal{Z}^f}{|\mathcal{Z}^f|}. \quad (2.37)$$

The focus of Sec. 4 will be to use Eq. 2.36 to extract information about R_D^f and δ_D^f , or equivalently, $\text{Re} \mathcal{Z}^f$ and $\text{Im} \mathcal{Z}^f$.

2.2. Decays to Self-Conjugate Final States

This section adapts the mixing formalism in Sec. 2 for the specific case of a self-conjugate final state. This applies when $f = \bar{f}$ up to particle ordering, and results in the following equalities:

$$\mathcal{B}(\mathbf{p}) \equiv \bar{\mathcal{A}}(\mathbf{p}) \quad \bar{\mathcal{B}}(\mathbf{p}) \equiv \mathcal{A}(\mathbf{p}) \quad (2.38)$$

In this step it is important to notice that the amplitudes $\bar{\mathcal{A}}(\mathbf{p})$ and $\bar{\mathcal{B}}(\mathbf{p})$ are evaluated at the phase space point \mathbf{p} , which is usually associated with a point in CP conjugate amplitudes $\mathcal{A}(\mathbf{p})$ and $\mathcal{B}(\mathbf{p})$. In fact, for a non self-conjugate final state, $\bar{\mathcal{A}}(\mathbf{p})$ and $\bar{\mathcal{B}}(\mathbf{p})$ are not defined. This subtle point brings an ambiguity to the definition of the integrated quantities \mathcal{A} , $\bar{\mathcal{A}}$ and \mathcal{Z}^f , because now the integral can run over Ω or $\bar{\Omega}$. For this reason an additional subscript is attached to these integrated quantities, indicating whether the integration volume is Ω or $\bar{\Omega}$.

For a self-conjugate final state, the following equalities hold for the integrated amplitudes and the complex interference parameter:

$$\mathcal{Z}_\Omega^f \equiv \mathcal{Z}_\Omega^{\bar{f}*} \quad \mathcal{A}_\Omega \equiv \bar{\mathcal{B}}_\Omega \quad \bar{\mathcal{A}}_\Omega \equiv \mathcal{B}_\Omega$$

These are obtained by substituting the equalities in Eq. 2.38 into the definitions of the integrated quantities in Eq. 2.16 and Eq. 2.17. The decay rates for a self-conjugate final state are then obtained by substituting these equalities into the rates shown in Eq. 2.25 and Eq. 2.27.

$$\Gamma(D^0(t) \rightarrow f)_\Omega \simeq e^{-\Gamma t} \left[\mathcal{A}_\Omega^2 \left(1 + \frac{y^2 - x^2}{4} (\Gamma t)^2 \right) + \bar{\mathcal{A}}_\Omega^2 \left(|\lambda|^2 \frac{x^2 + y^2}{4} (\Gamma t)^2 \right) + \mathcal{A}_\Omega \bar{\mathcal{A}}_\Omega \zeta(\mathcal{Z}_\Omega^f \lambda) (\Gamma t) \right] \quad (2.39)$$

$$\Gamma(\bar{D}^0(t) \rightarrow \bar{f})_{\bar{\Omega}} \simeq e^{-\Gamma t} \left[\bar{\mathcal{A}}_{\bar{\Omega}}^2 \left(1 + \frac{y^2 - x^2}{4} (\Gamma t)^2 \right) + \mathcal{A}_{\bar{\Omega}}^2 \left(\frac{1}{|\lambda|^2} \frac{x^2 + y^2}{4} (\Gamma t)^2 \right) + \bar{\mathcal{A}}_{\bar{\Omega}} \mathcal{A}_{\bar{\Omega}} \zeta(\mathcal{Z}_{\bar{\Omega}}^{f*} / \lambda) (\Gamma t) \right] \quad (2.40)$$

As discussed in Sec. 2, the following relations will hold in the case of no CP violation.

$$\mathcal{Z}_\Omega^f = \mathcal{Z}_{\bar{\Omega}}^{f*} \quad \mathcal{A}_\Omega = \bar{\mathcal{A}}_{\bar{\Omega}} \quad \lambda = 1$$

Where the final relation is subject to the phase convention that $\arg(\lambda) = \phi_{mix} = 0$ in the case of no CP violation. Substituting these into either

Eq. 2.39 or Eq. 2.40 we obtain the following rate:

$$\Gamma(D^0(t) \rightarrow f)_\Omega \simeq e^{-\Gamma t} \left[\mathcal{A}_\Omega^2 \left(1 + \frac{y^2 - x^2}{4} (\Gamma t)^2 \right) + \mathcal{A}_\Omega^2 \left(\frac{x^2 + y^2}{4} (\Gamma t)^2 \right) + \mathcal{A}_\Omega \mathcal{A}_{\bar{\Omega}} \zeta \left(\mathcal{Z}_\Omega^f \right) (\Gamma t) \right] \quad (2.41)$$

It is worth mentioning that although we use the complex interference parameter throughout our workings, it is easy to change to commonly used bin averaged sine and cosine, \mathbf{s}_i and \mathbf{c}_i defined in Eq. 2.18 [21].

$$\zeta \left(\mathcal{Z}_{\Omega_i}^f \right) = y c_i + x s_i \quad (2.42)$$

where Ω_i defines a subset of the kinematically allowed phase space volume.

3. Phase Conventions

The first phase convention we will fix is related to the $D^0 - \bar{D}^0$ mixing phase ϕ_{mix} , which, as already mentioned in the previous section, we set to zero in the case of no CP violation in the interference between mixing and decay, as is the usual convention. The second phase convention we need to resolve is related to the CP operator. In general

$$CP|D^0\rangle = e^{i\theta}|\bar{D}^0\rangle. \quad (3.1)$$

Because $(CP)^2 = 1$, there are two options for θ . Both are in common use:

$$\mathbf{HFAG} \quad [\theta = \pi]: \quad CP|D^0\rangle = -|\bar{D}^0\rangle \quad (3.2)$$

$$\mathbf{ADS} \quad [\theta = 0]: \quad CP|D^0\rangle = +|\bar{D}^0\rangle \quad (3.3)$$

The HFAG (Heavy Flavour Averaging Group) convention is usually used for charm analyses, whereas the ADS formalism related to extracting γ from $B \rightarrow DK$ decays follows the opposite convention. This difference in convention has of course no consequence in terms observable physics, but it affects the definition of several other parameters. We will first explore those related to mixing. In the case of no CP violation, the mass eigenstates (2.1) are the following:

$$\begin{aligned} |D_1\rangle &= |D^0\rangle + |\bar{D}^0\rangle, \\ |D_2\rangle &= |D^0\rangle - |\bar{D}^0\rangle. \end{aligned} \quad (3.4)$$

It is important to note that our choice of convention decides whether $|D_1\rangle$ or $|D_2\rangle$ is the CP even mass eigenstate, $|D_+\rangle$, or CP odd mass eigenstate $|D_-\rangle$. The mixing variables x and y are defined in terms of the CP eigenstates (or approximate CP eigenstates)

$$x = \frac{M_+ - M_-}{\Gamma}, \quad y = \frac{\Gamma_+ - \Gamma_-}{\Gamma}. \quad (3.5)$$

The formalism detailed in Sec. 2, with the mixing parameters defined in (2.6) applies to the HFAG convention. Changing this to the ADS convention implies a simultaneous changes $x \rightarrow -x$ and $y \rightarrow -y$.

The choice of convention also affects the complex interference parameter \mathcal{Z}^f . Considering Eq. 3.4, to ensure that the same physical CP even or CP odd state corresponds to the same wave function (up to a phase), the $|D^0\rangle$ and $|\overline{D}^0\rangle$ wavefunctions between the two conventions must be related by

$$\begin{aligned} |D^0\rangle_{\text{ADS}} &= e^{i\xi} |D^0\rangle_{\text{HFAG}} \\ |\overline{D}^0\rangle_{\text{ADS}} &= -e^{i\xi} |\overline{D}^0\rangle_{\text{HFAG}}, \end{aligned} \quad (3.6)$$

where ξ is an arbitrary phase. Recalling the definition of \mathcal{Z}^f :

$$\mathcal{Z}^f = \frac{\int_{\Omega} \langle f_{\mathbf{p}} | \hat{H} | D^0 \rangle \langle f_{\mathbf{p}} | \hat{H} | \overline{D}^0 \rangle^* d\mathbf{p}}{\sqrt{\int_{\Omega} |\langle f_{\mathbf{p}} | \hat{H} | D^0 \rangle|^2 d\mathbf{p} \int_{\Omega} |\langle f_{\mathbf{p}} | \hat{H} | \overline{D}^0 \rangle|^2 d\mathbf{p}}} \quad (3.7)$$

So, introducing convention-specific subscripts, in the HFAG convention this is:

$$\mathcal{Z}_{\text{HFAG}}^f = \frac{\int_{\Omega} \langle f_{\mathbf{p}} | \hat{H} | D^0 \rangle_{\text{HFAG}} \langle f_{\mathbf{p}} | \hat{H} | \overline{D}^0 \rangle_{\text{HFAG}}^* d\mathbf{p}}{\sqrt{\int_{\Omega} |\langle f_{\mathbf{p}} | \hat{H} | D^0 \rangle_{\text{HFAG}}|^2 d\mathbf{p} \int_{\Omega} |\langle f_{\mathbf{p}} | \hat{H} | \overline{D}^0 \rangle_{\text{HFAG}}|^2 d\mathbf{p}}}. \quad (3.8)$$

which we can now relate to the ADS-convention:

$$\begin{aligned}
\mathcal{Z}_{\text{ADS}}^f &= \frac{\int_{\Omega} \langle f_{\mathbf{p}} | \hat{H} | D^0 \rangle_{\text{ADS}} \langle f_{\mathbf{p}} | \hat{H} | \overline{D}^0 \rangle_{\text{ADS}}^* d\mathbf{p}}{\sqrt{\int_{\Omega} |\langle f_{\mathbf{p}} | \hat{H} | D^0 \rangle_{\text{ADS}}|^2 d\mathbf{p} \int_{\Omega} |\langle f_{\mathbf{p}} | \hat{H} | \overline{D}^0 \rangle_{\text{ADS}}|^2 d\mathbf{p}}} \\
&= \frac{\int_{\Omega} e^{i\xi} \langle f_{\mathbf{p}} | \hat{H} | D^0 \rangle_{\text{HFAG}} \left(-e^{-i\xi} \langle f_{\mathbf{p}} | \hat{H} | \overline{D}^0 \rangle_{\text{HFAG}}^* \right) d\mathbf{p}}{\sqrt{\int_{\Omega} |\langle f_{\mathbf{p}} | \hat{H} | D^0 \rangle_{\text{ADS}}|^2 d\mathbf{p} \int_{\Omega} |\langle f_{\mathbf{p}} | \hat{H} | \overline{D}^0 \rangle_{\text{ADS}}|^2 d\mathbf{p}}} \\
&= - \frac{\int_{\Omega} \langle f_{\mathbf{p}} | \hat{H} | D^0 \rangle_{\text{HFAG}} \langle f_{\mathbf{p}} | \hat{H} | \overline{D}^0 \rangle_{\text{HFAG}}^* d\mathbf{p}}{\sqrt{\int_{\Omega} |\langle f_{\mathbf{p}} | \hat{H} | D^0 \rangle_{\text{ADS}}|^2 d\mathbf{p} \int_{\Omega} |\langle f_{\mathbf{p}} | \hat{H} | \overline{D}^0 \rangle_{\text{ADS}}|^2 d\mathbf{p}}} \\
&= e^{-i\pi} \mathcal{Z}_{\text{HFAG}}^f \tag{3.9}
\end{aligned}$$

so the HFAG definition of \mathcal{Z}^f differs from the ADS definition by a phase change of π . To summarise: to convert the decay rate expressions in section 2, which are calculated in the HFAG convention with $CP|D^0\rangle = -|\overline{D}^0\rangle$, to the ADS convention with $CP|D^0\rangle = |\overline{D}^0\rangle$, requires the following variable transformation:

$$\begin{aligned}
x_{\text{ADS}} &= -x_{\text{HFAG}} \\
y_{\text{ADS}} &= -y_{\text{HFAG}} \\
\mathcal{Z}_{\text{ADS}}^f &= e^{-i\pi} \mathcal{Z}_{\text{HFAG}}^f. \tag{3.10}
\end{aligned}$$

In terms of the R_D^f and δ_D^f that are used to describe decays where $\mathcal{A} \ll \mathcal{B}$, this implies:

$$\begin{aligned}
R_{D,\text{ADS}}^f &= R_{D,\text{HFAG}}^f \\
\delta_{D,\text{ADS}}^f &= \delta_{D,\text{HFAG}}^f + \pi \tag{3.11}
\end{aligned}$$

while, in terms of the c_i and s_i variables used for decays to self-conjugate

final states, this implies:

$$\begin{aligned} c_i^{\text{ADS}} &= -c_i^{\text{HFAG}} \\ s_i^{\text{ADS}} &= -s_i^{\text{HFAG}}. \end{aligned} \quad (3.12)$$

4. Constraining the Coherence Factor with D Mixing

The coherence factor and average strong phase difference defined in [1] and given in Eq. 2.18 play an important role in the measurement of the CKM parameter γ . We will show here that even without the benefit of threshold data, meaningful constraints on R_D^f, δ_D^f can be obtained.

For simplicity, we assume no CP violation in charm in this section. If needed, it can be easily included using the formalism shown in Sec. 2. Without CP violation, the the time-dependent decay rate ratio of the suppressed versus the favoured D decay, given in Eq. 2.36, simplifies to:

$$r_\Omega(t) = r_{Df}^2 + r_{Df} R_D^f \left(y \cos(\delta_D^f) - x \sin(\delta_D^f) \right) \Gamma t + \frac{x^2 + y^2}{4} (\Gamma t)^2 \quad (4.1)$$

$$= r_{Df}^2 + r_{Df} \left(y \text{Re} \mathcal{Z}^f + x \text{Im} \mathcal{Z}^f \right) \Gamma t + \frac{x^2 + y^2}{4} (\Gamma t)^2, \quad (4.2)$$

where the two expressions above only differ in how the complex interference parameter \mathcal{Z}^f is expressed; either in polar or Cartesian coordinates. An analysis of the time-dependent decay rate ratio will, through the linear term of Eq. 4.2, provide a measurement of

$$b \equiv \Gamma r_{Df} R_D^f \left(y \cos(\delta_D^f) - x \sin(\delta_D^f) \right) = \Gamma r_{Df} \left(y \text{Re} \mathcal{Z}^f + x \text{Im} \mathcal{Z}^f \right) \quad (4.3)$$

The factor r_{Df} can be obtained in the same analysis from the 0^{th} order term of Eq. 2.36, and Γ has been measured very precisely [30]. Importantly, the measurements of the D mixing parameters x and y are now precise enough that we can translate a measurement of the linear term b to meaningful constraints in the $\text{Re} \mathcal{Z}^f - \text{Im} \mathcal{Z}^f$ plane, or equivalently the $R_D^f - \delta_D^f$ plane. Without taking into account any measurement uncertainties, a given value of b corresponds to a line in the $\text{Re} \mathcal{Z}^f - \text{Im} \mathcal{Z}^f$ plane defined by:

$$\text{Im} \mathcal{Z}^f = -\frac{y}{x} \text{Re} \mathcal{Z}^f + \frac{b}{x \Gamma r_{Df}}. \quad (4.4)$$

To illustrate the best constraints possible given the current uncertainties in

x and y , we consider first the limiting case of negligible uncertainties on any other parameter, in particular on b defined in Eq. 4.3. We use the following values and uncertainties for x, y , and their correlation coefficient $\rho_{x,y}$ [28]:

$$x = 0.63 \pm 0.19\%, \quad y = 0.75 \pm 0.12\%, \quad \rho_{x,y} = 0.043. \quad (4.5)$$

Figure 2 shows 1, 2 and 3σ confidence limits in the $Re\mathcal{Z}^f - Im\mathcal{Z}^f$ plane, obtained from likelihood scans using these inputs.

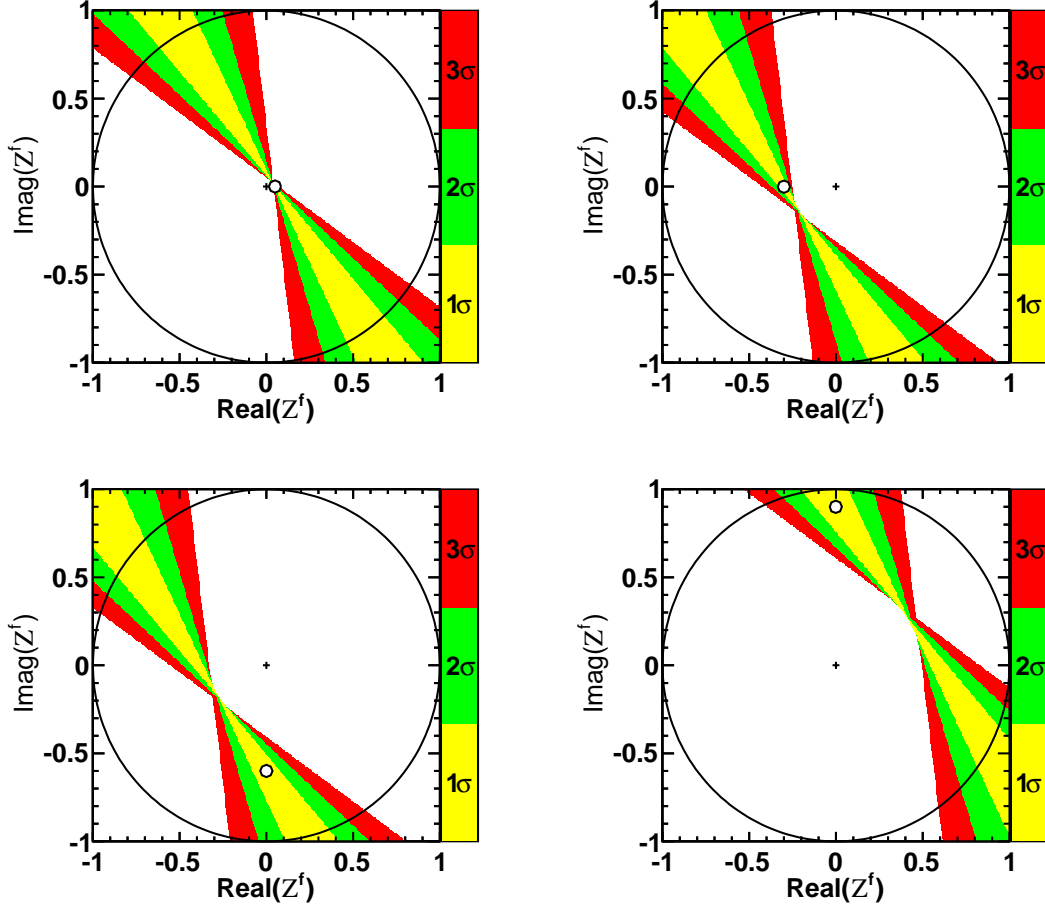


Figure 2: Illustration of constraints in the $ReZ^f - ImZ^f$ plane, with $Z^f = R_D^f e^{-i\delta_D^f}$, for different values of Z^f , taking into account the current uncertainties on x, y but ignoring, in this figure, other measurement uncertainties. The white filled circle indicates the central values of ReZ^f and ImZ^f used in the study.

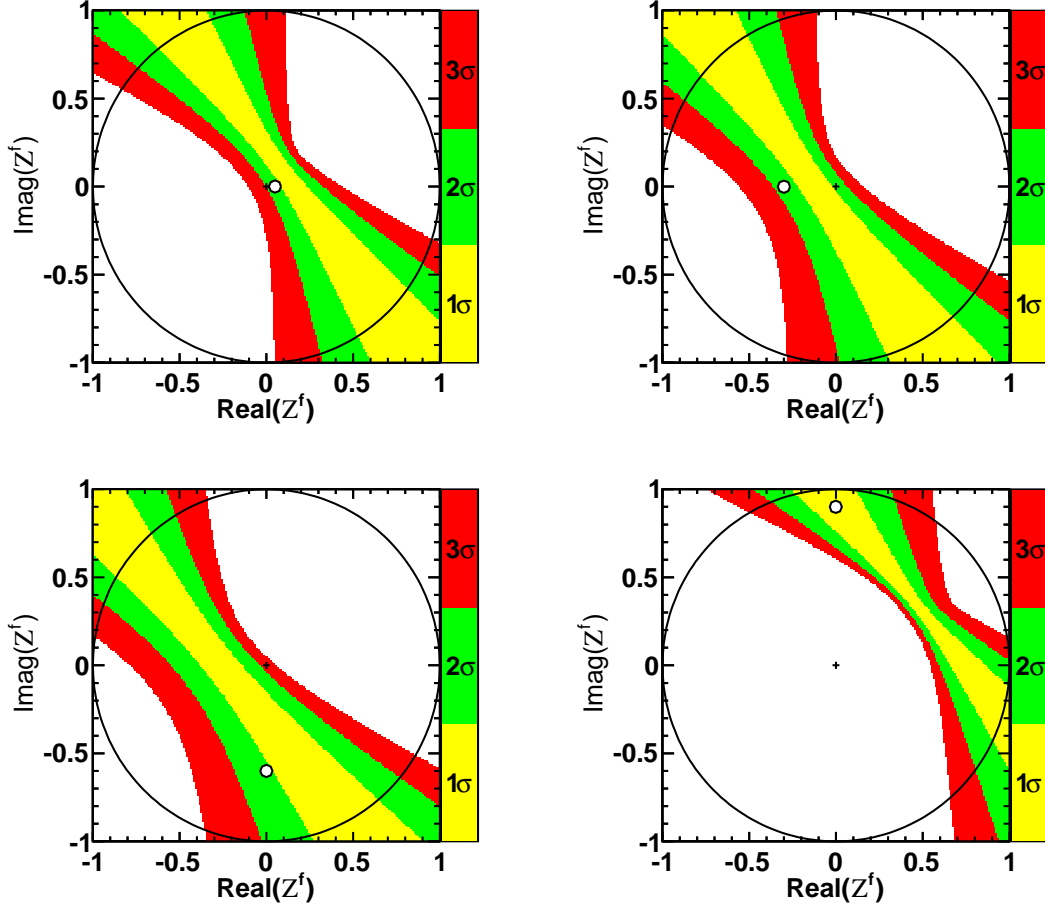


Figure 3: Illustration of constraints in the R_D^f, δ_D^f plane for different values of R_D, δ_B , found from 8 million simulated events, taking into account the current uncertainties on x, y . The white filled circle indicates the central values of ReZ^f and ImZ^f used in the study.

5. Simulation Study

We now estimate the constraints on \mathcal{Z}^f , or equivalently, R_D^f and δ_D^f for the four body decay $D \rightarrow K^+\pi^-\pi^+\pi^-$, where progress would be particularly beneficial, as statistical uncertainties on these parameters are quite large, while the channel plays an important role for measuring γ at LHCb. We base our study on plausible expected event yields in LHCb's 3fb^{-1} of data taken in 2011 and 2012.

For these studies, we generate simulated events according to the full expressions for the decay rates in Eqs. 2.20 - 2.23. To constrain \mathcal{Z}^f we fit the WS to RS ratio with the simplified expression in Eq. 2.36. This generating and fitting procedure has been shown to return unbiased results, which validates the approximations leading to Eq. 2.36.

To produce a simulated data sample, we take the values for mixing parameters given above [28]. We assume no CP violation in charm (i.e. $|\lambda| = 1$, $\phi_{mix} = 0$). As we anticipate this measurement to be made at LHCb, where hadronic charm decays are selected using a displaced vertex trigger and further lifetime biasing cuts, we apply a lifetime acceptance function based on that seen in [31]. Based on [32], and taking into account that for the WS mode a tighter selection might be necessary to control backgrounds, we estimate about 8 million RS + WS events in LHCb's 2011-2012 dataset. The exact fraction of WS events depends on the input parameters, in particular on R_D^f ; typically, 8 million RS + WS events correspond to about 27,000 WS events. Figure 3 shows likelihood scans based on 8 million simulated events for different R_D^f, δ_D^f values. Figure 4 shows the constraints on \mathcal{Z}^f in both polar and cartesian coordinates for for 8 million events generated using simulated using the CLEO-c central values $R_D^{K3\pi}$ and $\delta_D^{K3\pi}$ [18].

In order to demonstrate the benefit of the constraints on \mathcal{Z}^f from charm mixing when combined with charm threshold data, the likelihood scan shown in Fig. 4 is combined with the CLEO-c measurement. The results of this combination are shown in Fig. 5 and Fig. 6 for polar and cartesian coordinates respectively. The constraints improve significantly and look more Gaussian especially at the $\geq 2\sigma$ level. To quantify these improvements, the 68% and 95% confidence intervals are calculated. In order to compare our results with those shown in CLEO-c's publication [18], we follow the same procedures for obtaining one-dimensional confidence limits from the two-dimensional likelihood scan. CLEO-c use two different methods. Their 68% limits are based on the usual log-likelihood difference. The 95% limits, which reach

Best fit result (where available) with 68% confidence limits ($\Delta \log \mathcal{L}$)

	Simulation 8M evts	CLEO-c [18]	Combination
$R_D^{K3\pi}$	[0.28, 1.00]	$0.33^{+0.20}_{-0.23}$	$0.40^{+0.13}_{-0.11}$
$\delta_D^{K3\pi}$	[1.07, 3.77]	$1.99^{+0.46}_{-0.42}$	$2.03^{+0.33}_{-0.27}$

95% confidence limits ($\Delta \log \mathcal{L}$)

	Simulation 8M evts	CLEO-c [18]	Combination
$R_D^{K3\pi}$	[0.18, 1.00]	$0.33^{+0.37}_{-0.33}$	$0.40^{+0.27}_{-0.20}$
$\delta_D^{K3\pi}$	[0.88, 3.96]	–	$2.03^{+0.71}_{-0.52}$

Table 1: Constraints on $R_D^{K3\pi}$ and $\delta_D^{K3\pi}$ from simulated data, CLEO-c, and their combination at 68% and 95% confidence levels, calculated based on log-likelihood differences.

Bayesian 68% confidence limits

	Simulation 8M evts	CLEO-c [18]	Combination
$R_D^{K3\pi}$	[0.50, 1.00]	$0.33^{+0.17}_{-0.20}$	$0.40^{+0.13}_{-0.11}$
$\delta_D^{K3\pi}$	[1.54, 3.42]	$1.99^{+2.15}_{-1.71}$	$2.03^{+0.33}_{-0.30}$

Bayesian 95% confidence limits

	Simulation 8M evts	CLEO-c [18]	Combination
$R_D^{K3\pi}$	[0.27, 1.00]	$0.33^{+0.30}_{-0.33}$	$0.40^{+0.26}_{-0.20}$
$\delta_D^{K3\pi}$	[1.07, 3.83]	–	$2.03^{+0.74}_{-0.52}$

Table 2: Constraints on $R_D^{K3\pi}$ and $\delta_D^{K3\pi}$ from simulation, CLEO-c, and their combination at 68% and 95% confidence levels, calculated based on a Bayesian approach explained in the text, that takes into account the limited parameter space.

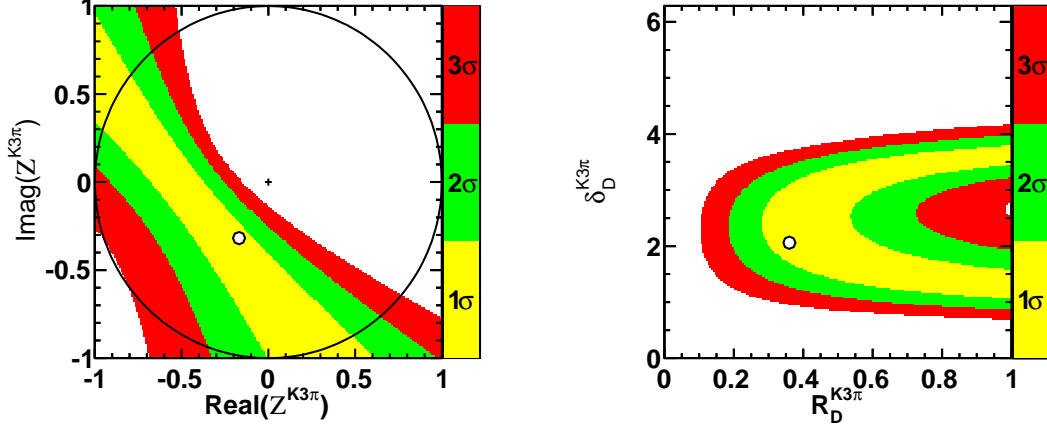


Figure 4: Illustration of constraints in the R_D^f, δ_D^f plane for toy data generated with the PDG central values. Both the Cartesian, and polar coordinates are shown. The white filled circle indicates the central values used to generate the toy data.

to the edge of parameter space, are based on a Bayesian approach. This involves performing a one-dimensional likelihood scan in each dimension. At each scan point in R_D^f the likelihood is evaluated at the value of δ_D^f that maximises the likelihood for this value of R_D^f , and vice versa for the δ_D^f scan. The resulting 1-dimensional scans are multiplied by a uniform prior in the physically allowed region, then integrated to obtain the 95% confidence limits. For comparison, we also apply this procedure for the 68% C.L. and confirm that it gives essentially the same result as the method based on the log-likelihood difference. This procedure for obtaining the Bayesian limits is illustrated in Fig. 7.

The numerical constraints found for the simulated D -mixing data by themselves, CLEO-c, and the combination are summarised in Tab. 1 and Tab. 2. The results indicate that the constraints obtained from charm mixing with $8M$ events could approximately halve the uncertainty in R_D^f , and significantly reduce the uncertainty on δ_D^f . While there is currently no constraint on δ_D^f at the 2σ level, and only a one-sided upper limit for the R_D^f , we obtain from a combination of our simulated data with the CLEO-c result, $\delta_D^f = 2.03_{-0.52}^{+0.74}$, and $R_D^f = 0.40_{-0.20}^{+0.26}$ at 95% confidence.

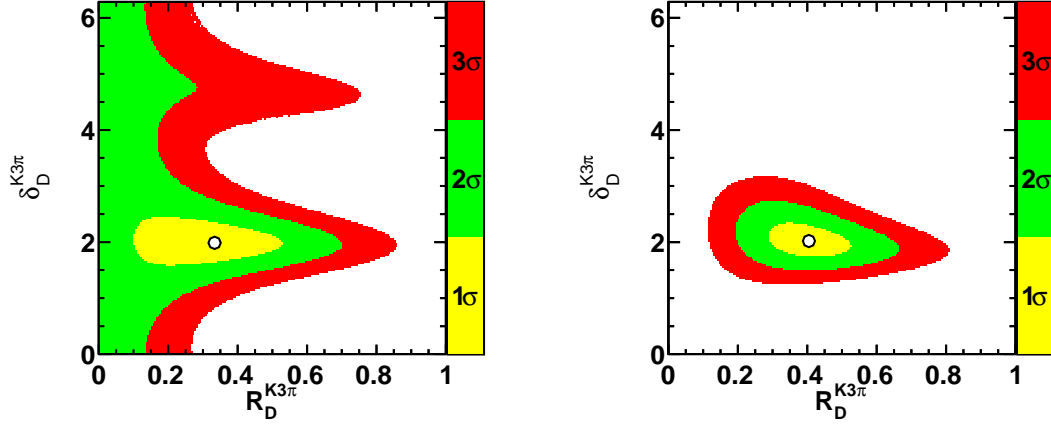


Figure 5: Left: An illustration of constraints in the R_D^f, δ_D^f plane set by CLEO-c. Right: Constraints set by combining CLEO-c constraints with the toy study constraints shown in Fig. 4. In both likelihood scans the white filled circle indicates the location with the greatest likelihood.

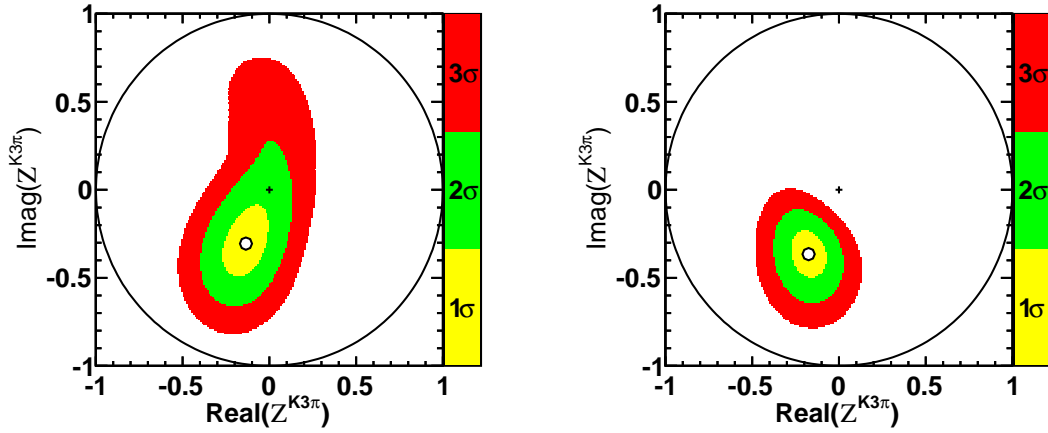


Figure 6: Left: An illustration of constraints in the $Re Z^f - Im Z^f$ plane set by CLEO-c. Right: Constraints set by combining CLEO-c constraints with the toy study constraints shown in Fig. 4. In both likelihood scans the white filled circle indicates the location with the greatest likelihood.

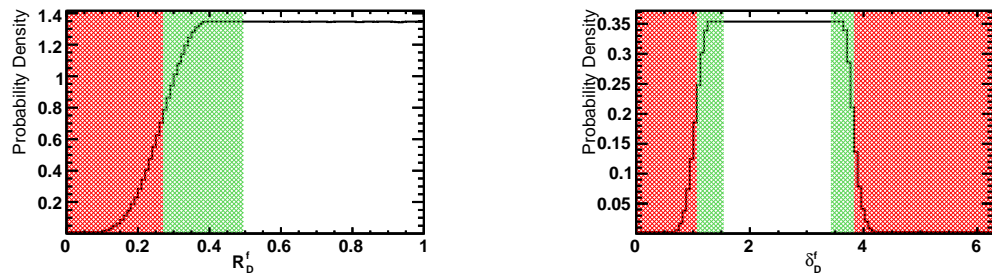


Figure 7: Illustration of the Bayesian 95% and 68% confidence intervals calculated from the simulated data sample shown in Fig. 4. The procedure is shown for both $R_D^{K3\pi}$ and $\delta_D^{K3\pi}$. The dark red hashed area indices the region excluded at 95% and the light green hashed area indicates the additional region excluded at 68%.

6. Conclusion

In this paper we present a novel method to constrain the complex interference parameter \mathcal{Z}^f . This parameter is related to the coherence factor R_D^f and the average strong phase difference δ_D^f defined in [1] through $\mathcal{Z}^f = R_D^f e^{-i\delta_D^f}$. For binned analyses and self-conjugate final states, the interference effects are usually expressed in terms of the c_i and s_i introduced in [2], which are related to \mathcal{Z}^f through $\mathcal{Z}_i^f = c_i + is_i$; the index i labels a bin in phase space, and we use the definition of c_i, s_i used in [15, 16].

These parameters play a crucial role in the precision measurement of γ from $B^- \rightarrow DK^-$ and similar decay modes. Previously, they could only be accessed at the charm threshold, which gives access to well-defined superposition states of D^0 and \overline{D}^0 . We introduce a new method of constraining \mathcal{Z}^f that can be applied to the huge charm samples available at LHCb, the B^0 factories, and their upgrades. We exploit the fact that D -mixing provides well-defined superposition states of D^0 and \overline{D}^0 in order to extract information about \mathcal{Z}^f . This input from charm mixing leads to a constraint that follows a line of slope $-y/x$ in the $Re\mathcal{Z}^f - Im\mathcal{Z}^f$ plane, where x and y are the charm mixing parameters; in practice, this line is spread out into an area as a result of measurement uncertainties. Our simulation studies indicate that LHCb, with its existing dataset, should be able to substantially improve the precision of these parameters for the decay $D \rightarrow K^-\pi^+\pi^-\pi^+$. Our results do not assume any improvements on external inputs to the analysis, such as the charm mixing parameters x and y and the constraints on \mathcal{Z}^f from the charm threshold. Such improvements could reduce the uncertainty on \mathcal{Z}^f even further. The improved measurement of \mathcal{Z}^f due to the input from charm mixing is expected to have a significant impact on the precision with which the CKM parameter γ can be measured at LHCb and its upgrade.

Acknowledgements

We thank our colleagues at CLEO-c and LHCb for their helpful input to this paper. We acknowledge support from CERN, the Science and Technology Facilities Council (United Kingdom) and the European Research Council.

References

- [1] D. Atwood, A. Soni, Role of charm factory in extracting CKM phase information via $B \rightarrow DK$, Phys.Rev. D68 (2003) 033003. [arXiv:hep-ph/0304085](#), [doi:10.1103/PhysRevD.68.033003](#).
- [2] A. Giri, Y. Grossman, A. Soffer, J. Zupan, Determining gamma using $B^\pm \rightarrow DK^\pm$ with multibody D decays, Phys.Rev. D68 (2003) 054018. [arXiv:hep-ph/0303187](#), [doi:10.1103/PhysRevD.68.054018](#).
- [3] M. Gronau, D. Wyler, On determining a weak phase from CP asymmetries in charged B decays, Phys.Lett. B265 (1991) 172–176. [doi:10.1016/0370-2693\(91\)90034-N](#).
- [4] M. Gronau, D. London, How to determine all the angles of the unitarity triangle from $B_d \rightarrow DK_s$ and $B_s^0 \rightarrow D\phi$, Phys.Lett. B253 (1991) 483–488. [doi:10.1016/0370-2693\(91\)91756-L](#).
- [5] D. Atwood, I. Dunietz, A. Soni, Enhanced CP violation with $B \rightarrow KD^0(\bar{D}^0)$ modes and extraction of the Cabibbo-Kobayashi-Maskawa Angle γ , Phys. Rev. Lett. 78 (1997) 3257–3260. [doi:10.1103/PhysRevLett.78.3257](#).
- [6] A. Giri, Y. Grossman, A. Soffer, J. Zupan, Determining γ using $B^\pm \rightarrow DK^\pm$ with multibody D decays, Phys. Rev. D 68 (2003) 054018. [doi:10.1103/PhysRevD.68.054018](#).
- [7] A. Poluektov, et al., Measurement of ϕ_3 with dalitz plot analysis of $B^\pm \rightarrow D^{(*)}K^\pm$ decays, Phys. Rev. D 70 (2004) 072003. [doi:10.1103/PhysRevD.70.072003](#).
- [8] J. Rademacker, G. Wilkinson, Determining the unitarity triangle gamma with a four-body amplitude analysis of $B^+ \rightarrow (K^+K^-\pi^+\pi^-)_D K^\pm$ decays, Phys.Lett. B647 (2007) 400–404. [arXiv:hep-ph/0611272](#), [doi:10.1016/j.physletb.2007.01.071](#).
- [9] A measurement of γ from a combination of $B^\pm \rightarrow DK^\pm$ analyses including first results using $2fb^{-1}$ of 2012 data (LHCb-CONF-2013-006).
- [10] R. Aaij, et al., A measurement of γ from a combination of $B^\pm \rightarrow Dh^\pm$ analyses submitted to Phys. Lett. B. [arXiv:1305.2050](#).

- [11] R. Aaij, et al., Observation of the suppressed ADS modes $B^\pm \rightarrow [\pi^\pm K^\mp \pi^+ \pi^-]_D K^\pm$ and $B^\pm \rightarrow [\pi^\pm K^\mp \pi^+ \pi^-]_D \pi^\pm$, Phys. Lett. B723 (2013) 44. [arXiv:1303.4646](#), [doi:10.1016/j.physletb.2013.05.009](#).
- [12] J. Lees, et al., Search for $b \rightarrow u$ Transitions in $B^\pm \rightarrow [K^\mp \pi^\pm \pi^0]_D K^\pm$ Decays, Phys.Rev. D84 (2011) 012002. [arXiv:1104.4472](#), [doi:10.1103/PhysRevD.84.012002](#).
- [13] J. Insler, et al., Studies of the decays $D^0 \rightarrow K_S^0 K^- \pi^+$ and $D^0 \rightarrow K_S^0 K^+ \pi^-$, Phys.Rev. D85 (2012) 092016. [arXiv:1203.3804](#), [doi:10.1103/PhysRevD.85.092016](#).
- [14] R. Aaij, et al., A model-independent Dalitz plot analysis of $B^\pm \rightarrow DK^\pm$ with $D \rightarrow K_S^0 h^+ h^-$ ($h = \pi, K$) decays and constraints on the CKM angle γ , Phys. Lett. B718 (2012) 43–55. [arXiv:1209.5869](#), [doi:10.1016/j.physletb.2012.10.020](#).
- [15] J. Libby, et al., Model-independent determination of the strong-phase difference between D^0 and $\bar{D}^0 \rightarrow K_{S,L}^0 h^+ h^-$ ($h = \pi, K$) and its impact on the measurement of the CKM angle γ/ϕ_3 , Phys.Rev. D82 (2010) 112006. [arXiv:1010.2817](#), [doi:10.1103/PhysRevD.82.112006](#).
- [16] R. A. Briere, et al., First model-independent determination of the relative strong phase between D^0 and $\bar{D}^0 \rightarrow K_s^0 \pi^+ \pi^-$ and its impact on the CKM Angle γ/ϕ_3 measurement, Phys.Rev. D80 (2009) 032002. [arXiv:0903.1681](#), [doi:10.1103/PhysRevD.80.032002](#).
- [17] D. M. Asner, et al., Determination of the $D^0 \rightarrow K^+ \pi^-$ Relative Strong Phase Using Quantum-Correlated Measurements in $e^+ e^- \rightarrow D^0 \bar{D}^0$ at CLEO, Phys.Rev. D78 (2008) 012001. [arXiv:0802.2268](#), [doi:10.1103/PhysRevD.78.012001](#).
- [18] N. Lowrey, et al., Determination of the $D^0 \rightarrow K^- \pi^+ \pi^0$ and $D^0 \rightarrow K^- \pi^+ \pi^+ \pi^-$ Coherence Factors and Average Strong-Phase Differences Using Quantum-Correlated Measurements, Phys.Rev. D80 (2009) 031105. [arXiv:0903.4853](#), [doi:10.1103/PhysRevD.80.031105](#).
- [19] I. Adachi, First measurement of ϕ_3 with a binned model-independent Dalitz plot analysis of $B^{+-} \rightarrow DK^{+-}$, $D \rightarrow K_s^0 \pi^+ \pi^-$ decay [arXiv:1106.4046](#).

- [20] S. Malde, G. Wilkinson, $D^0 - \bar{D}^0$ mixing studies with the decays $D^0 \rightarrow K_S^0 K^\mp \pi^\pm$, Phys.Lett. B701 (2011) 353–356. arXiv:1104.2731, doi:10.1016/j.physletb.2011.05.072.
- [21] A. Bondar, A. Poluektov, V. Vorobiev, Charm mixing in the model-independent analysis of correlated $D^0 \bar{D}^0$ decays, Phys.Rev. D82 (2010) 034033. arXiv:1004.2350, doi:10.1103/PhysRevD.82.034033.
- [22] T. Aaltonen, et al., Evidence for $D^0 - \bar{D}^0$ mixing using the CDF II Detector, Phys.Rev.Lett. 100 (2008) 121802. arXiv:0712.1567, doi:10.1103/PhysRevLett.100.121802.
- [23] M. Staric, et al., Evidence for $D^0 - \bar{D}^0$ Mixing, Phys.Rev.Lett. 98 (2007) 211803. arXiv:hep-ex/0703036, doi:10.1103/PhysRevLett.98.211803.
- [24] B. Aubert, et al., Evidence for $D^0 - \bar{D}^0$ Mixing, Phys.Rev.Lett. 98 (2007) 211802. arXiv:hep-ex/0703020, doi:10.1103/PhysRevLett.98.211802.
- [25] B. Aubert, et al., Measurement of $D^0 - \bar{D}^0$ mixing from a time-dependent amplitude analysis of $D^0 \rightarrow K^+ \pi^- \pi^0$ decays, Phys.Rev.Lett. 103 (2009) 211801. arXiv:0807.4544, doi:10.1103/PhysRevLett.103.211801.
- [26] B. Aubert, et al., Measurement of $D^0 - \bar{D}^0$ Mixing using the Ratio of Lifetimes for the Decays $D^0 \rightarrow K^- \pi^+$ and $K^+ K^-$, Phys.Rev. D80 (2009) 071103. arXiv:0908.0761, doi:10.1103/PhysRevD.80.071103.
- [27] R. Aaij, et al., Observation of $D^0 - \bar{D}^0$ oscillations, Phys. Rev. Lett. 110 (2013) 101802. arXiv:1211.1230, doi:10.1103/PhysRevLett.110.101802.
- [28] Y. Amhis, et al., Averages of B-Hadron, C-Hadron, and tau-lepton properties as of early 2012 arXiv:1207.1158.
- [29] C. A. Chavez, R. F. Cowan, W. Lockman, Charm meson mixing: An experimental review, Int.J.Mod.Phys. A27 (2012) 1230019. arXiv:1209.5806, doi:10.1142/S0217751X12300190.
- [30] J. Beringer, et al., Review of particle physics, Phys. Rev. D 86 (2012) 010001. doi:10.1103/PhysRevD.86.010001.
URL <http://link.aps.org/doi/10.1103/PhysRevD.86.010001>

- [31] R. Aaij, et al., Measurement of mixing and CP violation parameters in two-body charm decays, JHEP 04 (2012) 129. [arXiv:1112.4698](#), [doi:10.1007/JHEP04\(2012\)129](#).
- [32] R. Aaij, et al., Model-independent search for CP violation in $D^0 \rightarrow K^- K^+ \pi^- \pi^+$ and $D^0 \rightarrow \pi^- \pi^+ \pi^- \pi^+$ decays [arXiv:1308.3189](#).